Steam condensation in mini-channels: A benchmark of available correlations

Julie Jambert, Léa Pillemont, Sébastien Renaudière de Vaux, Florian Davin

14th International Topical Meeting on Nuclear Reactor Thermal-Hydraulics, Operation and Safety (NUTHOS-14)
Vancouver, BC, Canada, August 25 – 28, 2024

Steam condensation in mini-channels: A benchmark of available correlations

Julie Jambert and Léa Pillemont
ENSEEIHT

Sébastien Renaudière de Vaux
CEA Cadarache, Energy Division, IRESNE/DER/SESI
Corresponding Address
sebastien.renaudieredevaux@cea.fr

Florian Davin
CEA Saclay, Energy Division, ISAS/DM2S/STMF

ABSTRACT

This study takes place in the framework of the development of innovative heat exchangers. We consider a heat exchanger with vertical mini-channels (hydraulic diameter <3mm) operating in forced circulation, with pure steam at the inlet of the primary side. In such conditions, gravity and surface tension drive the condensation mechanism, but the latter effect is generally neglected in the modeling of the heat transfer coefficient. Indeed, condensation at mini-channel scale exhibits specific flow regimes that require dedicated modeling. Considerable effort has been done in the last two decades in order to model friction coefficients and heat transfer coefficients. Nevertheless, all the experimental studies took place with refrigerant fluids, whose properties significantly differ from those of steam. Therefore, transposition of previous work is delicate. A 1-dimensional model is used to investigate the effect of the closure laws on condensation and the results are compared with the results of the system-scale code CATHARE. In the latter model, surface tension effects are not taken into account. The results show that the decrease in hydraulic diameter favors quicker condensation, despite the increase in wall friction. Operating conditions are also explored. The results show a major influence of the heat transfer closure law on the results, e.g. the condensation length. This work highlights the lack of unicity in the available literature regarding steam condensation in innovative heat exchangers. Dedicated experimental work on steam is needed in the future.

KEYWORDS
Thermal hydraulics, steam condensation, mini-channels

1. INTRODUCTION AND PROBLEM MODELING

In order to extract heat in steam/water systems, two-phase heat exchangers are efficient ways of heating or cooling as they benefit from the large latent heat of the water $h_{lv} \approx 2300$ kJ/kg at room pressure. System-scale codes are used in research and industry and can help to the design of such components. However, validated closure laws are necessary to investigate these issues. In narrow channels specifically, boiling has received much more attention than condensing flows [1], and few condensation heat transfer laws are available. Moreover, recent reviews [2, 3] do not include validation based on experimental data obtained in steam/water configuration, but mostly on refrigerant fluids. Recent experiments with a refrigerant fluid pointed out that existing correlations exhibited large variations from experimental results [4]. It is then delicate to transpose these results to steam/water systems, as the physical properties significantly differ, sometimes from several orders of magnitude. One of the interest of having a robust correlation is the use

as a closure in thermal hydraulic system-scale codes. In this paper, potential closure laws for condensing steam/water flows in vertical narrow channels are investigated with a 1D model, and compared with results from the system-scale code CATHARE.

The situation considered here is schematically represented in Fig. 1. The overheated vapor enters the channel at T_{in} and exchanges with the wall at T_w. The vapor remains single-phase until the saturation temperature T_{sat} is reached, and then condensation starts, until only liquid remains, at the condensation length $z = L_{cond}$. The liquid is then further subcooled towards T_w. Here, the channel length is $L_{ch} = 4$ m throughout the study.

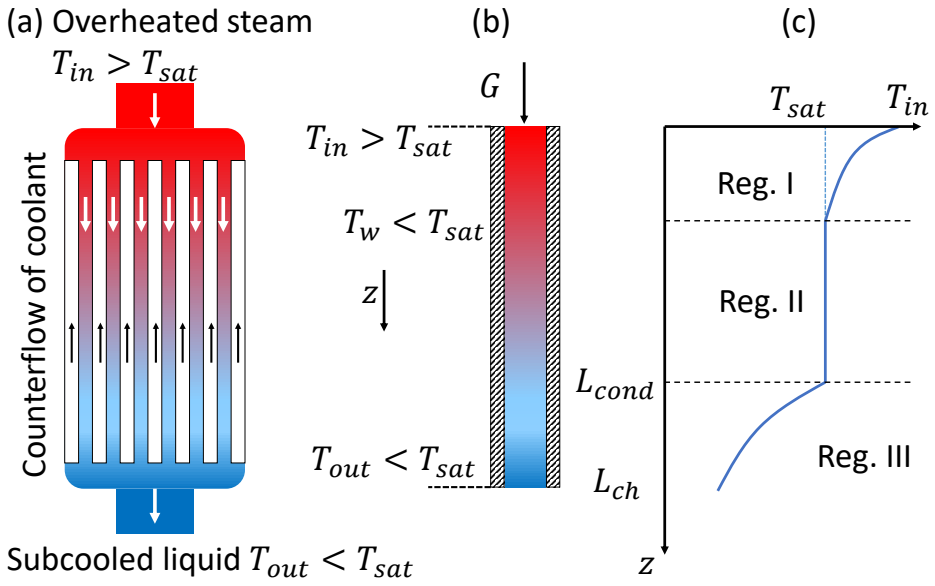

Figure 1. (a) General view of the considered configuration; (b) Close-up view at the single mini-channel scale; (c) Qualitative evolution of the temperature profile along the channel.

Qualitatively, the flow in the minichannel can be distinguished in three separate regions:

- Region I: single-phase overheated vapor;
- Region II: two-phase region;
- Region III: single-phase subcooled liquid.

In Reg. II, thermodynamic equilibrium is assumed, $T = T_{sat}$. The flow is considered incompressible in all regions. In particular, the physics involved in region II is not well known for narrow channels. At small scales, surface tension effects become predominant compared to gravitational and/or inertial effects. The typical drop size is given by the capillary length $l_c = \sqrt{\dfrac{\sigma}{(\rho_l - \rho_v)g}}$, with σ the surface tension, ρ_l and ρ_v the liquid and vapor densities, and g is acceleration of gravity. This characteristic length is used to build the Bond number Bo which compares the capillary effects to gravitational effects. We also introduce the We number, which compares surface tension effects to inertial effects. They are defined as:

$$Bo = \left(\frac{D}{l_c}\right)^2, \quad We = \frac{G^2 D}{\rho_v \sigma}, \tag{1}$$

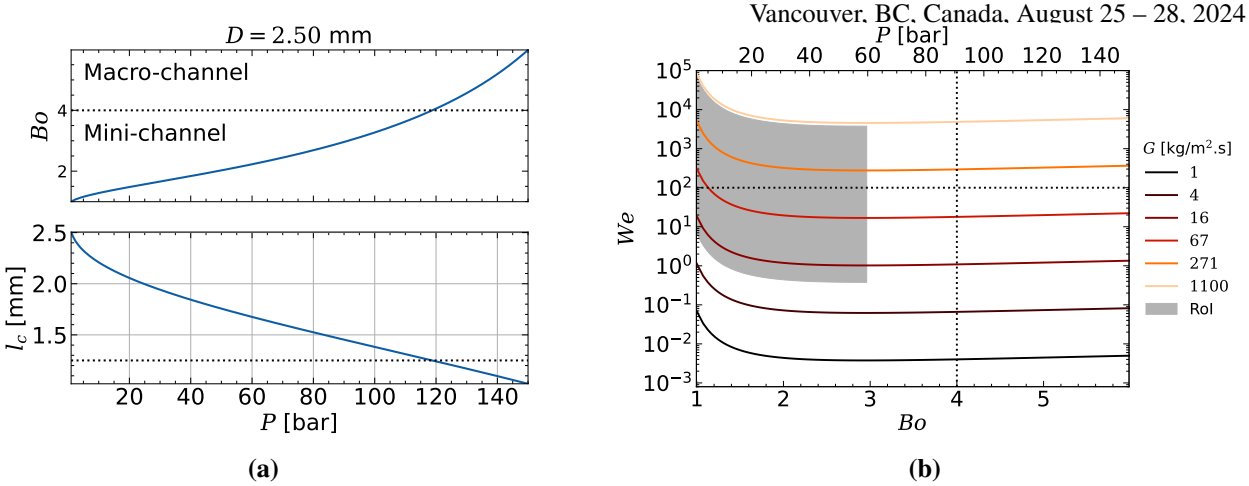

Figure 2. (a) Characteristic Bond number Bo and capillary length l_c with the pressure; (b) Typical evolution of Bo and We with P. The Region of Interest (RoI) is shaded.

where D is the channel hydraulic diameter, fixed at $D = 2.50$ mm, and G is the mass velocity. Several definitions have been proposed in the literature in order to classify channel types in macro-, mini– and micro-channels, based on their dimension or physical parameters. The most widely used are summarized in Tab. I. Kew and Cornell [5] proposed that below a critcal value of the Bond number $Bo = 4$, surface tension effects start to appear. This limit is close to the one proposed by Cheng and Wu [6], with $Bo = 3$. These authors introduce the micro-channels category, for $Bo < 0.05$. Kandlikar et al. [7] also propose three categories, but based on dimensional criteria, which may not be satisfactory, as it does not depend on fluid properties, nor flow conditions.

Table I. Channel classification.

Channel	**Kew and Cornell [5]**	**Kandlikar et al. [7]**	**Cheng and Wu [6]**
Macro-channel	$Bo > 4$	$D > 3$ mm	$Bo > 3$
Mini-channel	$Bo < 4$	200 μm $< D <$ 3 mm	$0.05 < Bo < 3$
Micro-channel	–	10μm $< D <$ 200μm	$Bo < 0.05$

In the following, mini-channels are considered as $Bo < 4$ for all cases, and all criteria give close classification in the current operating conditions. These definitions do not account for inertial effects. Shah [1] proposed that the critical Weber number, below which inertial effects are negligible compared to surface tension, is $We = 100$. The evolution of Bo with the operating pressure P is represented in Fig. 2a. The evolution with We is shown in Fig. 2b. At high pressure, $Bo > 4$, and the channel will behave similarly to a macro-channel. As P decreases, Bo also decreases and below $P = 100$ bar, $Bo < 4$ and the channel will behave as a mini-channel. The investigated pressure range here focuses on this region, shaded in grey in Fig. 2b. It is however seen that we consider values of the Weber number $We \ll 100$ and $We \gg 100$.

The flow equations are solved thanks to two models. First, a stationnary drift-flux model is developed to investigate the effect of the closure laws on the modeling of condensation, e.g. the condensation length L_{cond}. The results are compared with those of the system-scale code CATHARE [8]. A review of the literature is proposed in Section 2 to select the adequate correlations. Then, the drift-flux model and the CATHARE model are presented in Section 3. The results are presented and discussed in Section 4.

2. LITERATURE REVIEW

Pressure drop and condensation heat transfer are discussed in order to select adequate correlation models.

2.1. Two-phase pressure drop correlations

Numerous pressure drop correlations are found in the literature. Several pressure drop correlations were identified that focus on the desired mass flux, diameter range and pressure. The classical Lockhart and Martinelli model [9] is also investigated for comparison with more recent work [10–18].

2.2. Condensation heat transfer correlations

As for pressure drop, many condensation heat transfer laws are available in the literature. However, many focus on large diameters $D \gg 3$ mm , or large mass velocities $G \gg 100$ kg/m^2.s [1]. In the end, eight correlations are selected which cover the desired G and D [1, 10, 19–22].

For the heat transfer coefficient h, none of the proposed correlations depends on the wall subcooling. For the dependency of h with G and D, the characteristic scaling is given in Tab. II. Various dependencies are seen, but the exponents D are all negative, except for h from Ref. [20], meaning that larger channels impede heat transfer. An opposite conclusion is drawn for the G dependency, as all exponents are positive and an increase in heat transfer is expected.

However, this observations are not relevant for the condensation length L_{cond}. Indeed, the enthalpy balance in region II reads:

$$\dot{m} h_{lv} = D \int_0^{L_{cond}} q''(z) dz \tag{2}$$

with the heat flux density $q'' = -h\Delta T_w = -h(T_{sat} - T_w) < 0$, and the mass flowrate $\dot{m} = G \times A_c$.The cross-sectional area is $A_c = \pi D^2/4$. For the correlations used here, the leading order terms that play on h can be extracted. The dependence of h with G and D is summarized in Tab. II. Using these leading order terms in (2) leads to:

$$L_{cond} \propto \frac{GD}{f(D,G)\Delta T_w}, \tag{3}$$

with $f(G,D)$ a function that depends on the selected model, but not on ΔT_w. It is seen that in all cases, a drastic effect of the wall subcooling is expected as $L_{cond} \propto \Delta T_w^{-1}$. For all closure laws, L_{cond} increases with G and D, but with various exponents. The leading order scalings are summarized in Tab. II and suggest that total condensation is reached quicker for narrow channels, at low mass flux. It is also worth noticing that for most of the correlations, equation (2) cannot be analytically integrated given the proper expression for h, as it depends on pressure losses.

3. NUMERICAL METHODS

3.1. Mixture flow model

We present here the steady-state drift flux model developed for this study. The fluid properties are determined using the `CoolProp` Python library [25].

Table II. Scaling of h and L_{cond}.

Correlation	**Dependency to D and G**	**Effect on L_{cond}**
Dobson and Chato [19]	$h \propto D^{-0.2}G^{0.8}$	$L_{cond} \propto D^{1.2}G^{0.2}$
Thome et al. [20]	$h \propto D^{0.24}G^{0.12}(\log G)^{-0.62}$	$L_{cond} \propto D^{0.76}G^{0.88}(\log G)^{0.62}$
Wang [21]	$h \propto D^{-0.3208}G^{0.6792}$	$L_{cond} \propto D^{1.3208}G^{0.3208}$
Dorao and Fernandino [22]	$h \propto D^{-0.2}G^{0.48}$	$L_{cond} \propto D^{1.2}G^{0.52}$
Kim and Mudawar [10]	$h \propto D^{-0.31}G^{0.69}$	$L_{cond} \propto D^{1.31}G^{0.31}$
Shah [1, 23]	$h \propto D^{-0.2}G^{0.8}$ (other possible regimes)	$L_{cond} \propto D^{1.2}G^{0.2}$
Chen et al. [24]	$h \propto D^{-0.6}G^{0.4}$ (assuming turbulent regime)	$L_{cond} \propto D^{1.6}G^{0.6}$

3.1.1. Single-phase regions : I and III

In regions I and III, the fluid is single-phase vapor (I) or single-phase liquid (III). We assume that the heat transfer coefficient is given by the Dittus-Boelter law [26, 27] :

$$h = 0.023\frac{\lambda_k}{D}Re_k^{0.8}Pr^{0.4}. \tag{4}$$

The index k refers to the fluid phase, liquid (l) or vapor (v). The heat conductivity is λ_k and the Reynolds and Prandtl number of phase k are defined as:

$$Re_k = \frac{GD}{\mu_k}; \quad Pr_k = \frac{\nu_k}{\kappa_k}, \tag{5}$$

with μ_k the dynamic viscosity, ν_k and κ_k the viscous and heat diffusivities of each phase. The 1D steady-state enthalpy balance over each single-phase region reads:

$$\frac{dT}{dz} + \frac{1}{\delta_k}(T - T_w) = 0, \tag{6}$$

with $\delta_k = Gc_{p,k}D/h$ a characteristic cooling length, where $c_{p,k}$ is the heat capacity of phase k. Equation (6) is promptly solved as:

$$\text{Region I: } T(z) = T_w - (T_w - T_{in})\exp(-z/\delta_v), \tag{7}$$

$$\text{Region III: } T(z) = T_w - (T_w - T_{sat})\exp(-(z - L_{cond})/\delta_l). \tag{8}$$

It is assumed that region I ends when $T = T_{sat}$ and that region III starts when the vapor mass fraction is $x < 10^{-6}$.

3.1.2. Two-phase region: Region II

Here, it is assumed that both phases are at thermodynamic equilibrium, $T = T_{sat}$. The following model is based on the Martinelli–Nelson method [28–30]. This approach is close to the drift-flux model. The mixture is considered as a single homogeneous phase with a prescribed slip velocity. However some terms

are neglected. The simplified stationnary equations for mass, momentum and enthalpy read:

$$\frac{d}{dz}\left[(1-\alpha)\rho_l U_l + \alpha\rho_v U_v\right] = \frac{dG}{dz} = 0 \tag{9}$$

$$\frac{dP}{dz} = \left(\frac{dP}{dz}\right)_a + \left(\frac{dP}{dz}\right)_f + \left(\frac{dP}{dz}\right)_g \tag{10}$$

$$\frac{d}{dz}\left[(1-\alpha)\rho_l h_l U_l + \alpha\rho_v h_v U_v\right] = \frac{q'' P_w}{A_c}, \tag{11}$$

with α the void fraction, U_l and U_v the liquid and vapor velocities (defined later in Eq. (14)), h_l and h_v the liquid and vapor enthalpies. The wetted perimeter P_w is taken to be equal to the channel diameter, $P_w = D$. The accelerational and gravitational pressure losses are given by:

$$\left(\frac{dP}{dz}\right)_a = -G^2 \frac{d}{dz}\left(\frac{1}{\rho_m}\right), \quad \left(\frac{dP}{dz}\right)_g = \rho_m g \tag{12}$$

and the mixture density is $\rho_m = [(1-\alpha)\rho_l + \alpha\rho_v]$. Equation (11) can be rewritten as:

$$G h_{l_v} \frac{dx}{dz} = \frac{q'' P_w}{A_c} = \frac{4q''}{D}. \tag{13}$$

The liquid and vapor velocities are defined as a function of the mass fraction x:

$$U_l = \frac{G(1-x)}{\rho_l(1-\alpha)}, \quad U_v = \frac{Gx}{\rho_v \alpha}. \tag{14}$$

In [28], the void fraction– vapor quality is obtained assuming a homogeneous flow. Thom [29] introduces a slip ratio between the vapor and liquid, that depends on the pressure only. Here, we consider that the void fraction-vapor quality is given by:

$$\alpha = \frac{x}{C_0\left(x + (1-x)\dfrac{\rho_v}{\rho_l}\right) + \dfrac{\rho_v u_d}{G}}, \tag{15}$$

with the drift-flux parameters C_0 and u_d given by:

$$C_0 = 1.2 - 0.2\sqrt{\frac{\rho_v}{\rho_l}}, \quad u_d = 0.32\sqrt{\frac{Dg(\rho_l - \rho_v)}{\rho_l}}. \tag{16}$$

A comparison with drift parameters from Bestion [8] did not show significant differences on the results.

The two-phase frictional pressure drop is computed following Lockhart and Martinelli [9]:

$$\left(\frac{dP}{dz}\right)_f = \left(\frac{dP}{dz}\right)_l \Phi_l^2. \tag{17}$$

The parameter Φ_l^2 was correlated by Chisolm [31] as:

$$\Phi_l^2 = 1 + \frac{C}{X} + \frac{1}{X^2}, \quad X^2 = \frac{(dP/dz)_l}{(dP/dz)_v} \tag{18}$$

where $(dP/dz)_k$ are the equivalent single-phase pressure drops, computed as:

$$\left(\frac{dP}{dz}\right)_k = \frac{-2 f_k \rho_k \alpha_k^2 U_k^2}{D}, \tag{19}$$

with α_k the volume fraction of phase k. The friction coefficient is computed as:

$$f_k = \begin{cases} 16/Re'_k & \text{if } Re'_k \leq 10^3, \\ 0.079(Re'_k)^{-0.25} & \text{otherwise,} \end{cases} \tag{20}$$

with $Re'_k = \alpha_k \rho_k U_k D/\mu_k$ the Reynolds number considering only phase k. Several authors proposed closure laws for the fitting parameter C. This is discussed in Section 4.2. The wall heat transfer is computed as follows:

$$q'' = -h\Delta T_w, \tag{21}$$

with $\Delta T_w = T_{sat} - T_w$ and h the heat transfer coefficient from the correlations.

The model is solved with a first order upstream finite difference scheme. It was verified that numerical convergence was achieved. It is noticeable that the energy and momentum equations are only coupled by the h term, which in some cases depends on the pressure losses. Therefore it is chosen for consistency to always solve the full model. Moreover, the pressure losses prediction are of importance for natural circulation systems, which are also of interest.

3.2. CATHARE model

The CATHARE code is a two-fluid six-equation model at the system-scale [8]. The condensation heat transfer is given by a ponderation between two condensation models, i.e. Chen et al. [24] and Shah [23], valid for large diameters $D > 8$ mm. Pure steam with a given T_{in} and G is imposed at the inlet. The mesh convergence is discussed in Section 4.1.

4. RESULTS AND DISCUSSION

In this section, we first discuss the numerical convergence. Then we discuss the pressure loss correlation, and the heat transfer coefficient values given by the various selected models. Finally the effect on the condensation length is reported.

4.1. Parameters plan and mesh convergence

The parameter plan is as follow. Four operating pressures are investigated, $P = 70, 15, 7, 1$ bar and at three differents mass fluxes $G = 10, 100, 1000$ kg/m^2.s. Two wall subcoolings are investigated, $\Delta T_w = T_{sat} - T_w = 5, 30$°C. For all cases, the inlet vapor temperature is $T_{in} = T_{sat} + 1$°C, in order to have a negligible single-phase vapor regime (Region I) compared to the two-phase regime (Region II).

A mesh convergence study was also performed, as shown in Fig. 3, for three meshes with respectively $N = 26, 41, 81$ regularly spaced nodes. Qualitatively, the profiles are similar, especially when the condensation length L_{cond} is above 1 m. For lower L_{cond}, the difference is larger, because of the steepness of the void fraction profiles. However, due to the qualitative aspect of this work, it is considered that sufficient convergence is achieved with $N = 81$.

For the mixture flow model, a convergence study has also been performed. As it is a steady 1D model, the nodes number is not a limiting parameter and $N = 4000$ was chosen. The relative difference in L_{cond} between $N = 4000$ and 20000 was equal to machine zero.

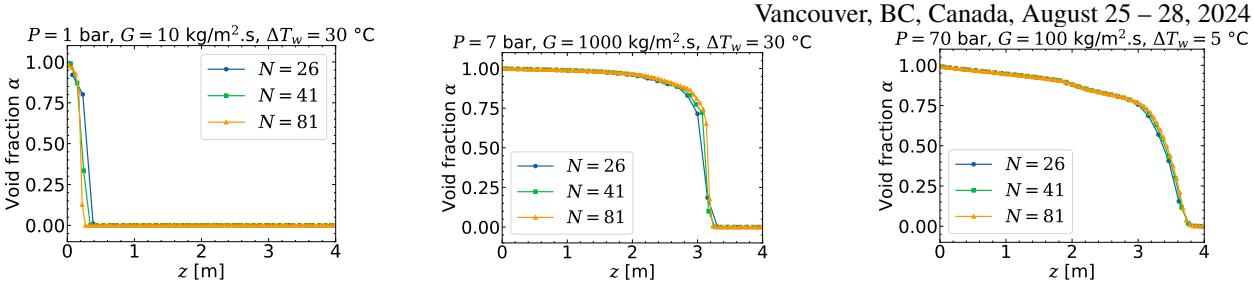

Figure 3. Mesh convergence for the CATHARE model. Three typical profiles of void fraction are shown here.

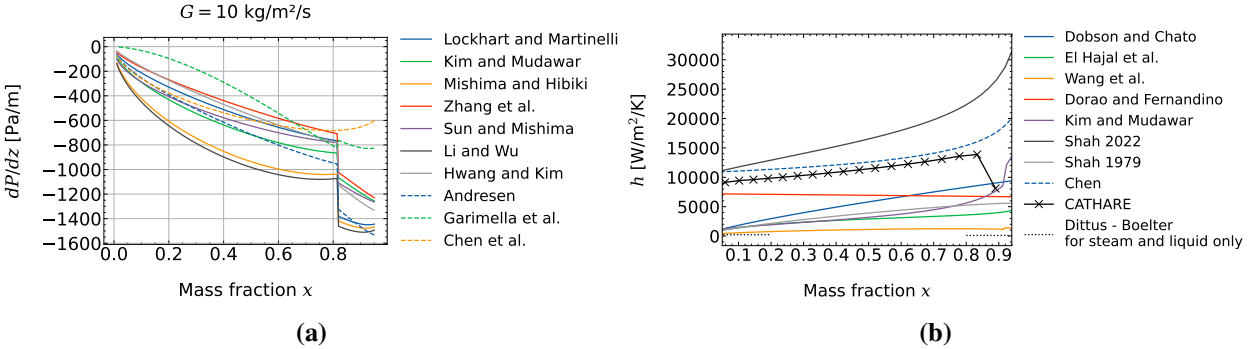

Figure 4. Effect of (a) the pressure drop closure law; (b) the heat transfer closure law.

4.2. Pressure drop correlation

The effect of the pressure drop correlation on the frictional pressure gradient is shown in Fig. 4a. First, it is observed that for all cases, dP/dz increases (in absolute value) with x. A jump is observed for some closure laws around $x = 0.8$. This is due to regime changes. Although the dP/dz values largely differ, no significant effect on the output L_{cond} was noticed. This is likely due to the forced circulation conditions. The Lockhart and Martinelli model is chosen as it is one of the most commonly used.

4.3. Heat transfer coefficient

The values of h are represented in Fig. 4b as a function of x for the selected closure laws. All correlations show an increase with x and some display jumps around $x = 0.8$, also due to regime changes. It is striking that the h values display a huge dispersion, with more than one order of magnitude of difference depending on the correlation. In this case, a major effect of the closure law on L_{cond} is expected. It is moreover observed that CATHARE follows the Chen et al. correlation [24], as expected.

4.4. Condensation length

Void fraction profiles are shown in Fig. 5 for $\Delta T_w = 30°C$ and $5°C$. The void fraction profiles are steep, due to the void fraction-vapor quality relation (15), as the density ratio $\rho_l/\rho_v \approx 10^3$. In the Martinelli-Nelson model, the initial value of α at $z = 0$ is slightly lower than 1, because of Eq. (15). The void fraction then decreases until it reaches $\alpha = 0$ at $z = L_{cond}$. A large dispersion in L_{cond} is observed. For example, in Fig. 5a,

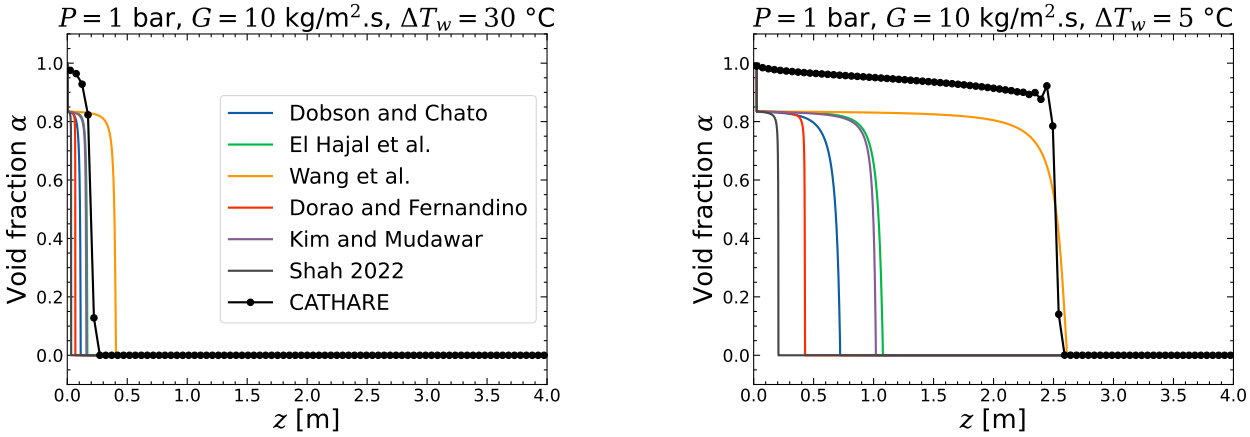

(a) **(b)**

Figure 5. Void fraction profiles: Effect of external wall temperature.

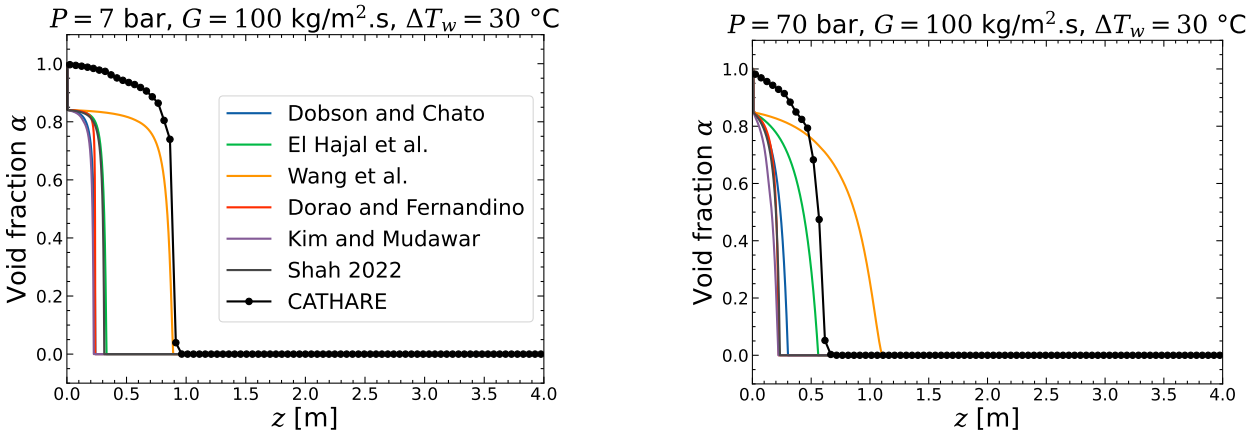

(a) **(b)**

Figure 6. Void fraction profiles: Effect of pressure.

$0.05\text{m} \leq L_{cond} \leq 0.4\text{m}$, which represents approximately an order of magnitude. Moreover, it is found that the selected models usually predict a smaller L_{cond} than CATHARE, except for [21] which always predict similar or larger values of L_{cond} than other models.

The increase in operating pressure smooths the void fraction profiles, as shown in Fig. 6. This effect is observed both with the Martinelli–Nelson model and the CATHARE model. This is due to the change in physical properties, in particular the density ratio ρ_l/ρ_v decreases with the pressure. However, the effect on L_{cond} is limited.

The ratio of the upper and lower quartile of the L_{cond} values to the median value for the considered correlations is shown in Fig. 9. Although the results have no statistical meaning with only seven correlations, it shows trends in the dispersion of L_{cond}, in relative values. First, it is observed that the results are independent on ΔT_w. This is due to (2), as h values are independent on ΔT_w. Second, the decrease in dispersion is favored by (i) the decrease in operating pressure, (ii) the increase in G. At 70 bar and $G = 10\text{kg/m}^2\text{.s}$, the typical dispersion of L_{cond} is given by a factor 2, whereas at 1 bar and $G \geq 100$ kg/m^2.s, the characteristic relative

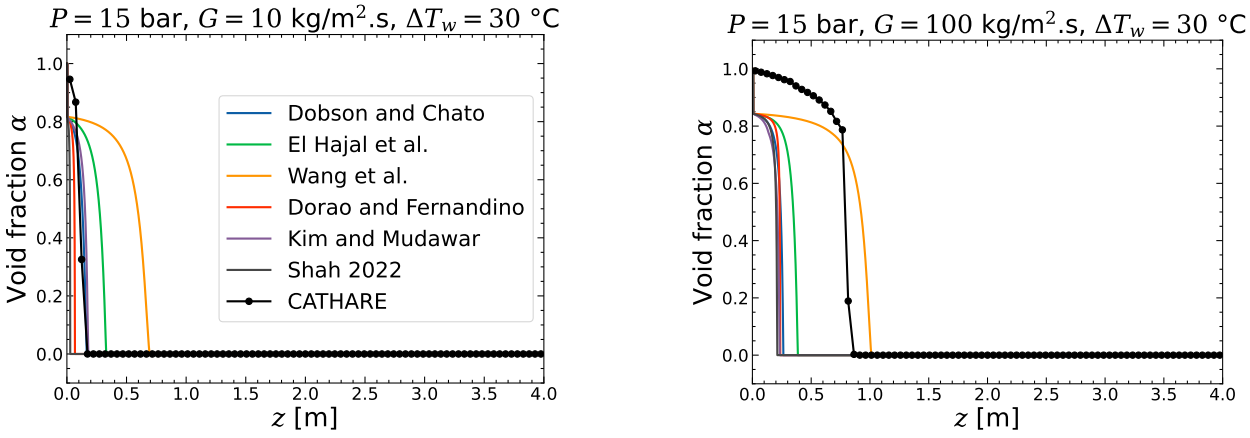

(a) **(b)**

Figure 7. Void fraction profiles: Effect of G.

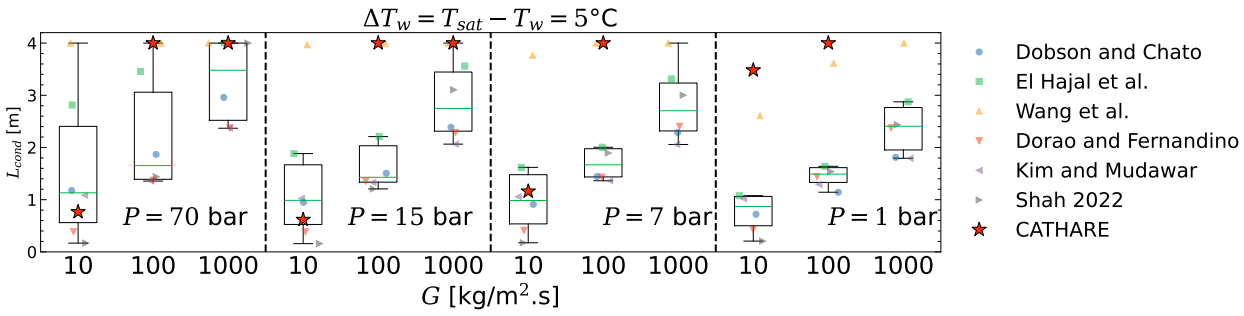

(a) $\Delta T_w = 5$°**C.**

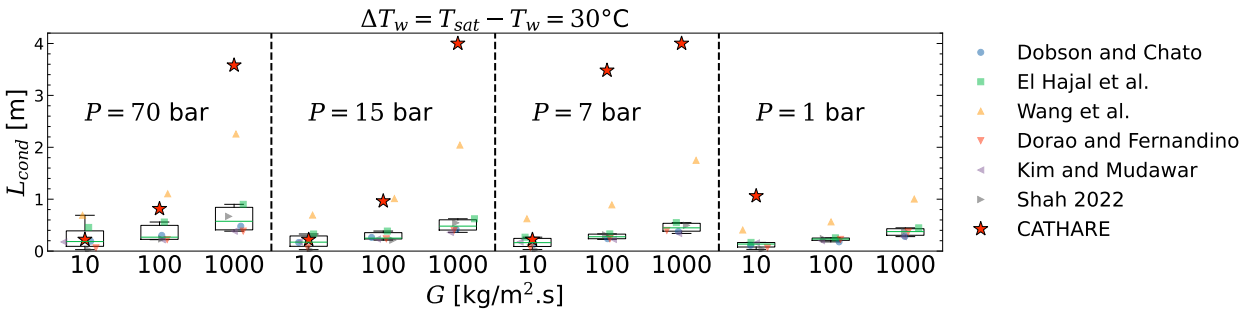

(b) $\Delta T_w = 30$°**C.**

Figure 8. Boxplots of the L_{cond} value from chosen closure laws. The red stars represent the value from CATHARE.

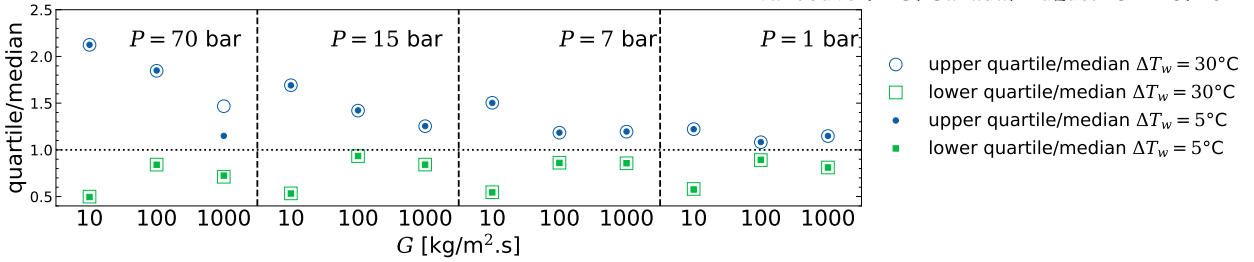

Figure 9. Ratio of the upper and lower quartiles to the median value of L_{cond}.

dispersion is lower than 10%.

However, when ΔT_w decreases, the absolute value of L_{cond} increases (see Eq. (2) and Fig. 8), and raises issues in the framework of heat exchanger design.

5. CONCLUSION AND PROSPECTS

Steam condensation in narrow channels was investigated using the Martinelli–Nelson method and the system-scale code CATHARE. Several closure laws for the pressure drop and the condensation heat transfer were reviewed and tested.

First, the consistency of the leading order scaling is observed. Despite variations in the exponent, all correlations show an decrease of h with the pipe diameter, and an increase of h with the mass flux. The variations however lead to large dispersion in the condensation length, by a factor 10 in the worst cases. In the context of the design of innovative heat exchangers, available data is not sufficient and dedicated experiments with steam are necessary to adapt a condensation heat transfer model.

At this state, it is difficult to select one of the available correlations to design millemeter-sized heat exchangers to be implemented in a system-scale code. Indeed, all correlations were determined with other fluids as steam/water, and display large variations for the same operating conditions. More work on the subject is necessary. In particular, dedicated experiments with water and steam are required.

ACKNOWLEDGMENTS

Authors acknowledge Catherine Colin for suggestions that improved the quality of the work.

REFERENCES

1. M. M. Shah, *Two-Phase Heat Transfer*, John Wiley & Sons (2021).

2. K. El Kadi, F. Alnaimat, and S. Sherif, "Recent advances in condensation heat transfer in mini and micro channels: A comprehensive review," *Applied Thermal Engineering*, **197**, pp. 117412 (2021).

3. M. M. Shah, "Improved correlation for heat transfer during condensation in mini and macro channels," *International Journal of Heat and Mass Transfer*, **194**, pp. 123069 (2022).

4. M. Beaumale, P. Lavieille, F. Topin, and M. Miscevic, "Simultaneous high-accuracy measurements of local heat transfer and phase distribution during convective condensation using non intrusive diagnostic tools," *Experimental Thermal and Fluid Science*, **141**, pp. 110801 (2023).

5. P. A. Kew and K. Cornwell, "Correlations for the prediction of boiling heat transfer in small-diameter channels," *Applied thermal engineering*, **17** (8-10), pp. 705–715 (1997).

6. P. Cheng and H. Wu, "Mesoscale and microscale phase-change heat transfer," *Advances in heat transfer*, **39**, pp. 461–563 (2006).

7. S. G. Kandlikar and W. J. Grande, "Evolution of microchannel flow passages–thermohydraulic performance and fabrication technology," *Heat transfer engineering*, **24** (1), pp. 3–17 (2003).

8. D. Bestion, "The physical closure laws in the CATHARE code," *Nuclear Engineering and design*, **124** (3), pp. 229–245 (1990).

9. W. Lockhart, "Proposed correlation of data for isothermal two-phase, two-component flow in pipes," *Chemical engineering progress*, **45** (1), pp. 39–48 (1949).

10. S.-M. Kim and I. Mudawar, "Flow condensation in parallel micro-channels–Part 2: Heat transfer results and correlation technique," *International Journal of Heat and Mass Transfer*, **55** (4), pp. 984–994 (2012).

11. K. Mishima and T. Hibiki, "Some characteristics of air-water two-phase flow in small diameter vertical tubes," *International journal of multiphase flow*, **22** (4), pp. 703–712 (1996).

12. W. Zhang, T. Hibiki, and K. Mishima, "Correlations of two-phase frictional pressure drop and void fraction in mini-channel," *International Journal of Heat and Mass Transfer*, **53** (1-3), pp. 453–465 (2010).

13. L. Sun and K. Mishima, "Evaluation analysis of prediction methods for two-phase flow pressure drop in mini-channels," *Proc. International Conference on Nuclear Engineering*, volume 48159, pp. 649–658 (2008).

14. W. Li and Z. Wu, "A general correlation for adiabatic two-phase pressure drop in micro/mini-channels," *International Journal of Heat and Mass Transfer*, **53** (13-14), pp. 2732–2739 (2010).

15. Y. W. Hwang and M. S. Kim, "The pressure drop in microtubes and the correlation development," *International journal of heat and mass transfer*, **49** (11-12), pp. 1804–1812 (2006).

16. U. C. Andresen, *Supercritical gas cooling and near-critical-pressure condensation of refrigerant blends in microchannels*, PhD thesis, Mechanical Engineering, Georgia Institute of Technology, 2006.

17. S. Garimella, A. Agarwal, and J. D. Killion, "Condensation pressure drops in circular microchannels," *Proc. International Conference on Nanochannels, Microchannels, and Minichannels*, volume 41642, pp. 649–656 (2004).

18. Y. Chen, K.-S. Yang, Y.-J. Chang, and C.-C. Wang, "Two-phase pressure drop of air–water and R-410A in small horizontal tubes," *International journal of multiphase flow*, **27** (7), pp. 1293–1299 (2001).

19. M. K. Dobson and J. C. Chato, "Condensation in smooth horizontal tubes," (1998).

20. J. R. Thome, J. El Hajal, and A. Cavallini, "Condensation in horizontal tubes, part 2: new heat transfer model based on flow regimes," *International journal of heat and mass transfer*, **46** (18), pp. 3365–3387 (2003).

21. W.-W. W. Wang, T. D. Radcliff, and R. N. Christensen, "A condensation heat transfer correlation for millimeter-scale tubing with flow regime transition," *Experimental Thermal and Fluid Science*, **26** (5), pp. 473–485 (2002).

22. C. A. Dorao and M. Fernandino, "Simple and general correlation for heat transfer during flow condensation inside plain pipes," *International Journal of Heat and Mass Transfer*, **122**, pp. 290–305 (2018).

23. M. M. Shah, "A general correlation for heat transfer during film condensation inside pipes," *International Journal of heat and mass transfer*, **22** (4), pp. 547–556 (1979).

24. S. Chen, F. Gerner, and C. Tien, "General film condensation correlations," *Experimental Heat Transfer An International Journal*, **1** (2), pp. 93–107 (1987).

25. I. H. Bell, J. Wronski, S. Quoilin, and V. Lemort, "Pure and Pseudo-pure Fluid Thermophysical Property Evaluation and the Open-Source Thermophysical Property Library CoolProp," *Industrial & Engineering Chemistry Research*, **53** (6), pp. 2498–2508 (2014); https://doi.org/10.1021/ie4033999.

26. F. Dittus and L. Boelter, "Heat transfer in automobile radiators of the tubular type," *International communications in heat and mass transfer*, **12** (1), pp. 3–22 (1985).

27. R. H. Winterton, "Where did the Dittus and Boelter equation come from?," *International journal of heat and mass transfer*, **41** (4-5), pp. 809–810 (1998).

28. R. T. Martinelli and D. Nelson, "Prediction of pressure drop during forced-circulation boiling of water," *Transactions of the American Society of Mechanical Engineers*, **70** (6), pp. 695–702 (1948).

29. J. Thom, "Prediction of pressure drop during forced circulation boiling of water," *International journal of heat and mass transfer*, **7** (7), pp. 709–724 (1964).

30. J.-M. Delhaye, "Thermohydraulique des réacteurs," in *Thermohydraulique des réacteurs*, EDP sciences, (2008).

31. D. Chisholm, "A theoretical basis for the Lockhart-Martinelli correlation for two-phase flow," *International Journal of Heat and Mass Transfer*, **10** (12), pp. 1767–1778 (1967).